

MASS OUTFLOW IN MOLECULAR CLOUDS: A NEW PHASE IN THE EVOLUTION OF NEWLY-FORMED STARS?

R. Genzel

Dept. of Physics, University of California, Berkeley

D. Downes

Institut de Radio Astronomie Millimétrique, Grenoble

I. INTRODUCTION

Molecular gas with velocity dispersions exceeding 100 km s^{-1} toward dense, interstellar clouds was discovered by microwave observers about a decade ago. It has now been established that this high velocity gas is a result of violent mass outflows (winds) originating from T-Tau stars, compact infrared sources or ultra-compact HII regions at the cores of the clouds. The mass outflow phenomena occur in regions of star formation covering five orders of magnitude in luminosity, and are of long duration ($\sim 10^4 \text{ y}$). The observations suggest that violent mass loss is a new, important phase in the pre-main sequence evolution of newly-formed stars more massive than a few solar masses. The impact of the flows on the energy balance and dynamical stability of molecular clouds may be substantial. This review is mainly a summary of the observational facts, and gives a description of the physical conditions in an outflow zone. The impact of the flows on molecular clouds is discussed. Recent reviews of the outflow phenomena can also be found in (1, 2, 3,).

II. OBSERVATIONS

1. High Velocity Molecular Gas

High velocity molecular gas was first discovered as "high velocity, maser emission" in the 22 GHz rotational transition of H_2O (e.g., 4). Fig. 1 is an H_2O spectrum toward the luminous HII region W49 which shows many maser lines spread over a total velocity range of about 500 km s^{-1} . An interpretation of the high velocity H_2O maser features in terms of mass outflow came as early as 1972 in the perceptive paper by Strel'nitskii and Syunyaev (5). As proposed by those authors, every one of the maser lines in the W49 spectrum corresponds to a compact cloulet ($d \sim 10^{13}$ to 10^{14} cm) of dense gas ($n_{\text{H}_2} \sim 10^9$ to 10^{11} cm^{-3}), moving at space velocities up to a few hundred km s^{-1} . However, the importance of the high velocity motions in dense molecular clouds was not widely recognized until 1976, when high-quality spectra of the $J=1 \rightarrow 0$ CO line at 115 GHz toward the Orion molecular cloud clearly showed non-Gaussian wings (the

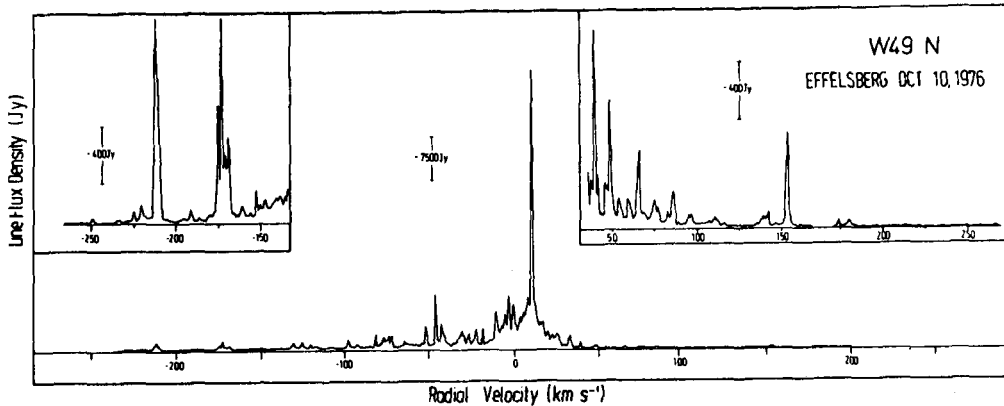


Fig. 1: Spectrum of the $6_{16}-5_{23}$ transition of H_2O at 22 GHz toward the distant molecular cloud W49 (from measurements with the 100-m Effelsberg telescope by the authors). There are about 400 maser features spread over 500 km s^{-1} in radial velocity (see top left and right insets).

"plateau"), extending out to $\pm 60 \text{ km s}^{-1}$ from the line center (Fig. 2)(6,7) In retrospect, however, these wings were already visible in the discovery spectrum of this line, as well as in some other microwave molecular lines (8, 9, 10). High velocity gas near interstellar clouds per se was actually discovered much earlier (11, 12) in the optical spectra of Herbig-Haro objects. As will be shown below, the Herbig-Haro phenomenon is only one of many manifestations of the outflowing matter in regions of star formation.

2. Shocked Gas

Line emission from vibrationally excited molecular hydrogen in the near infrared (Fig. 3; ref. 13) gives a second, independent indication of violent activity in the Orion molecular cloud. Since the $v=1$ state of H_2 is about 6000 K above the ground state, and since the detected emission lines are quite intense ($\sim 1 L_{\odot}$ in the $v=1-0$, $S(1)$ line alone), a substantial component of very hot, molecular gas must be present toward the center of the Orion molecular cloud. Work by several groups since the first detection on a large number of ro-vibrational and rotational lines of H_2 at $\lambda \leq 12 \mu\text{m}$ has established that the hot hydrogen has a range of temperatures between 1000 and 3000 K, and that hydrogen densities of at least 10^5 cm^{-3} are required (e.g. 14-20). At high spectral resolution, the lines have a total velocity width (full width zero power, FWZP) $> 100 \text{ km s}^{-1}$, comparable with the full range of the CO, SiO and H_2O emission (21, 18). Further evidence for this hot molecular gas are CO emission lines in high rotational states (J up to 34) in the submillimeter and far-infrared wavelength bands, as well as far-infrared emission lines of OH and neutral, atomic oxygen (Fig. 4, refs. 22-24).

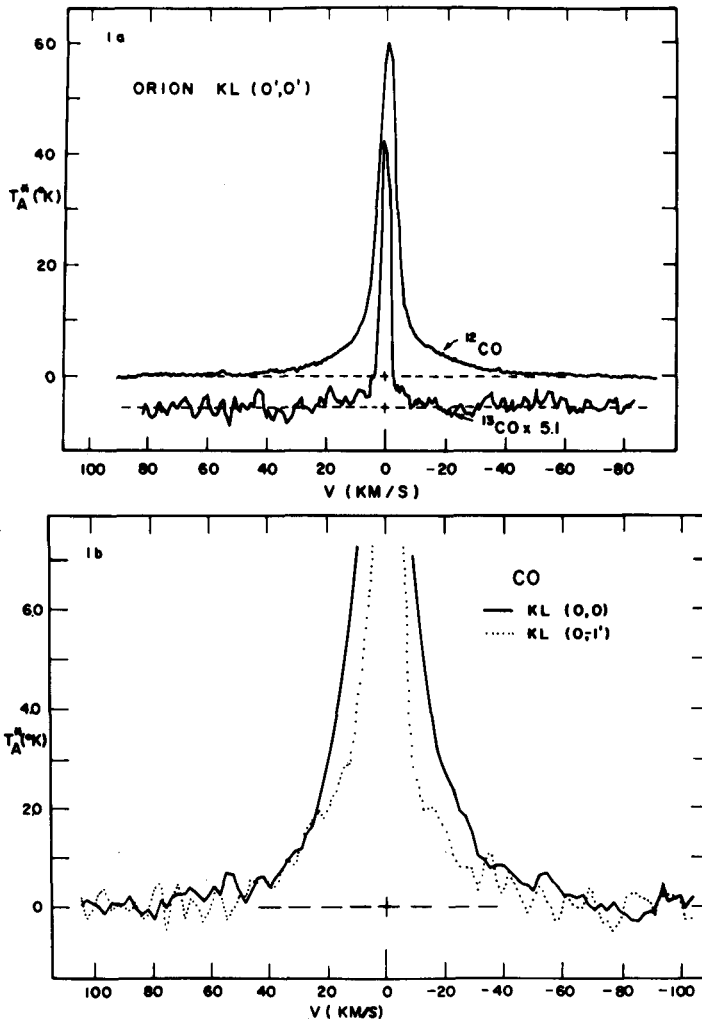


Fig. 2: Spectrum of the $J=1-0$ line of CO at 115 GHz toward the Orion-KL region (from (6)). There is CO emission in non-Gaussian wings (the "plateau") over a total range $\geq 100 \text{ km s}^{-1}$ (see bottom profile which emphasizes the weak emission). The ^{13}CO line (top) does not show a significant plateau suggesting that the high velocity emission is not very optically thick.

The most likely excitation mechanism for the hot gas are shock waves due to the supersonic motions (the sound speed in molecular gas with $T \leq 100 \text{ K}$ is $< 1 \text{ km s}^{-1}$). The measurement of the intensities of the

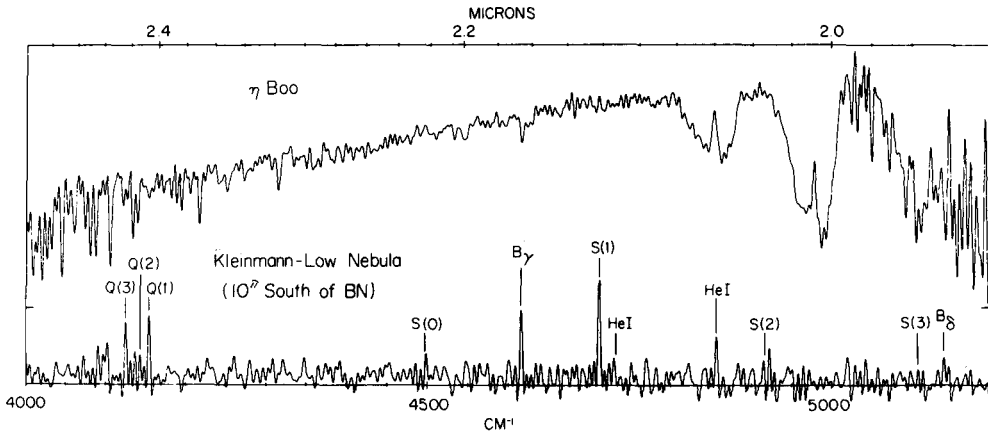


Fig. 3: 2 μ m spectrum of the Orion-KL region (bottom, from 13). The top spectrum is a calibration spectrum of the atmospheric transmission toward the star η Boo. In addition to the hydrogen recombination lines $B\gamma$, $B\delta$ from the foreground Orion HII region, there are emission lines from vibrationally excited, molecular hydrogen (S(0) to S(3), Q(1) to Q(3)). The emission probably comes from hot, shocked molecular gas in the Orion-KL region.

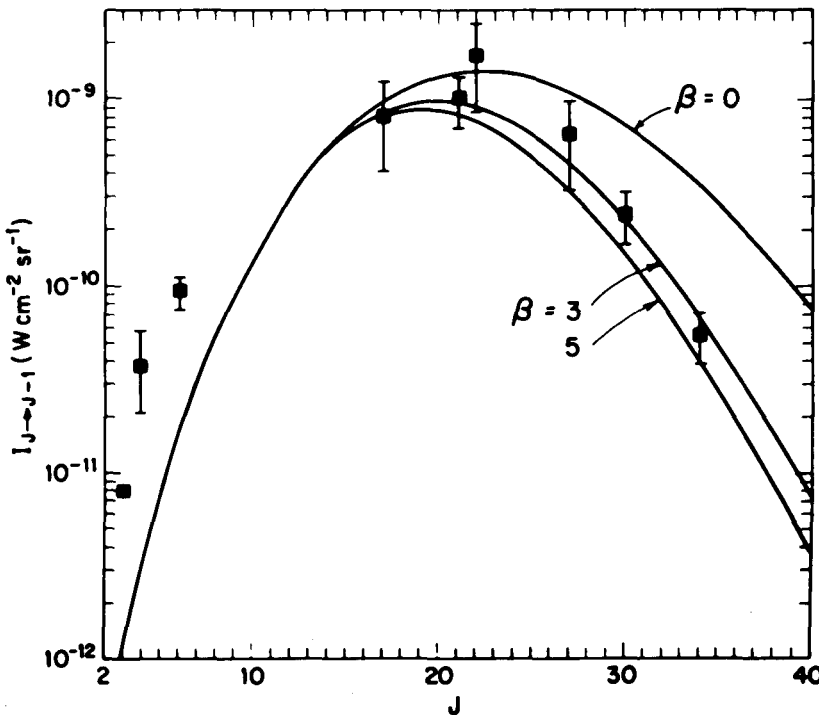


Fig. 4: Intensities of CO rotational lines in the submm and far infrared regions (from 22, 23, 24, 75, 95-97). The solid curves are models for the shocked gas in Orion-KL (from 29). The curves are plotted for three different choices of the CO collisional cross sections.

infrared lines, together with a theoretical model of the shock excitation is then a powerful tool to quantitatively constrain the physical characteristics, such as: density and temperature structure, molecular abundances, near infrared extinction, shock speed(s), total momentum and energy contained in the motions, etc. A problem for the early models was that pure gas dynamic shocks at shock speeds suggested by the line widths ($>20 \text{ km s}^{-1}$) implied very high post-shock temperatures ($>>10^3 \text{ K}$) and hence, dissociation of most of the molecules in the hot post-shock layers (25, 26). Furthermore, to quantitatively match the line intensities, unreasonably high, pre-shock densities ($>10^7 \text{ cm}^{-3}$) were required. More recently, this problem has probably been solved by the suggestion (27) that the interaction of a magnetic field with ions in the pre-shock gas could attenuate the shock, and produce a softer compression of the gas, with larger column densities of medium-temperature gas. The calculations now successfully account for most of the observed lines with the following set of parameters: Magnetic fields of $\sim 1 \text{ mG}$, pre-shock density $2\text{--}7 \times 10^5 \text{ cm}^{-3}$ and shock speeds between 20 and 40 km s^{-1} . From the comparison between H_2 and CO lines, a CO/H_2 abundance of $1\text{--}3 \times 10^{-4}$ is derived (28, 29).

3. Location and Kinematics of the High Velocity Gas

Fig. 5 shows the spatial distribution of the $2 \mu\text{m}$ H_2 quadrupole emission (dashed), CO "plateau" emission (dotted circle) and H_2O maser features (dots), superposed on the contours of $20 \mu\text{m}$ continuum emission from warm dust (14, 30-32). The high velocity/hot gas is distributed around ($\sim 0.1 \text{ pc}$) and roughly centered on the infrared nebula at the core of the Orion molecular cloud. It is almost certainly not associated with the Trapezium OB cluster, or the Orion HII region which are centered about $1'$ SE of the BN-KL region.

The positions of the H_2O maser features can be measured to milli-arcsec accuracy, and proper motions of about 40 maser cloudlets have been determined (32). The data unambiguously show that the H_2O features are expanding away (schematically indicated by arrows in Fig. 5) from a common centroid located between the compact infrared sources IRc4 (the "KL" nebula) and IRc2 (cross in Fig. 5). The distributions and kinematics of the high velocity gas also show that the outflow has been continuous over the time scale $R/v \sim 10^3 \text{ yr}$, and is not due to a single explosion.

4. The Momentum Problem

From the column density of CO high velocity gas (with an adopted CO/H_2 ratio), and from the luminosity of the hot molecular emission in Orion-KL (100 to 200 L_\odot , after correction for extinction), the integrated parameters of the flowing and swept-up gas can be estimated (32-36). The total mass in the high velocity gas is $3 M_\odot$, the mass loss rate is $3 \times 10^{-3} M_\odot \text{ yr}^{-1}$ (for a dynamical time scale of 10^3 y), the momentum transport, Mv , is $3 \times 10^{39} \text{ erg cm}^{-1}$, and the total mechanical luminosity, $\frac{1}{2} Mv^2$, is $10^3 L_\odot$. Hence, the mechanical luminosity in the gas motions is only a small fraction of the total radiation luminosity

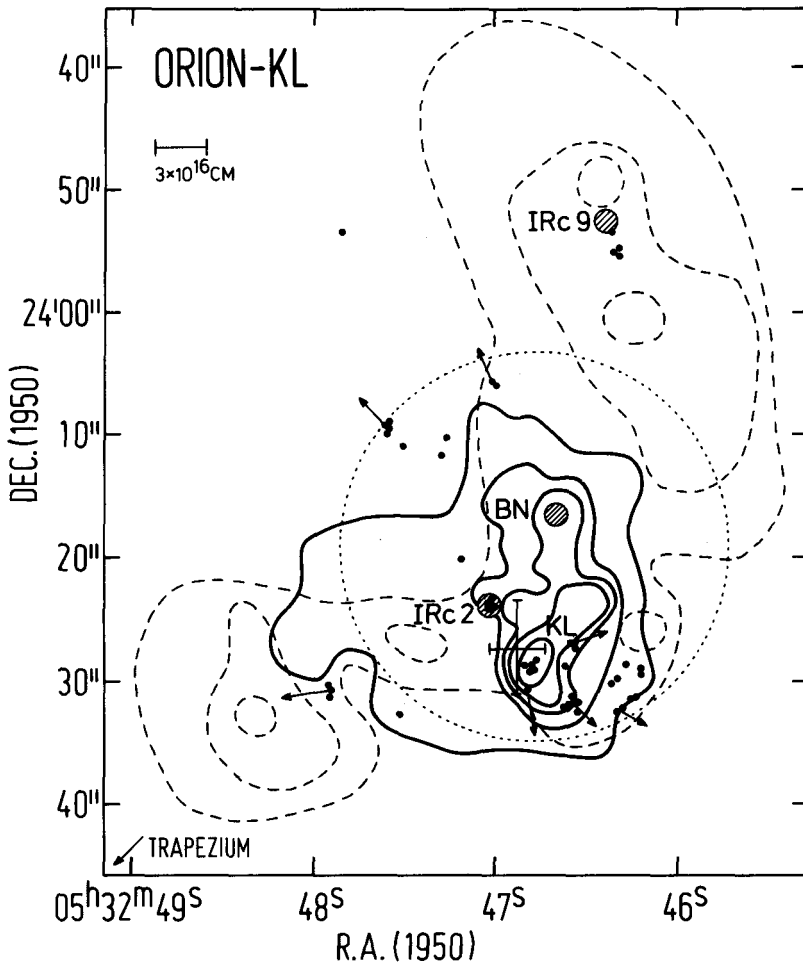


Fig. 5: Distribution of the hot and high velocity gas in the Orion-KL region, superposed on the contours of $20\ \mu\text{m}$ dust emission (from 33). Dashed contours give the integrated intensity of the $v=1-0\ S(1)$ line of H_2 (14). Dots are the positions of H_2O masers, and arrows schematically indicate their proper motions (32). The thin cross is the best fit centroid of the outflowing H_2O masers. The dotted circle indicates the size (FWHM) of the CO plateau source (6, 7, 30, 31, 75).

of the infrared cluster ($10^5 L_\odot$). However, the momentum in the flow is much larger than that provided by the radiation field:

$$(\dot{M}v)_{\text{FLOW}} c/L_{\text{RAD}} \approx 20$$

Although the estimate of $(\dot{M}v)_{\text{Flow}}$ is uncertain by more than a factor of two in either direction, this discrepancy is probably significant. Hence, the Orion-KL outflow cannot be driven by radiation pressure in single scattering (34-36, $\dot{M}v_{\text{SS}} \leq L/c$). If the infrared opacity of dust in the acceleration zone were large ($\tau_{\text{IR}} > 10$), multiple scattering of the photons may enhance the momentum transferred to the dust by τ_{IR} times the single scattering value (37, 31) and may then account for the observed momentum. Although such high infrared opacities in the envelope of IRC2 are not inconsistent with the observational data, a realistic, quantitative calculation of the radiative transport is not available yet.

Alternatively, the outflow(s) may not be driven by radiation pressure. Instabilities of the envelopes due to a large angular momentum of the collapsed protostar, or the presence of a companion may be attractive possibilities. Mass loss rates of $\sim 10^{-4} M_{\odot} \text{ y}^{-1}$ and expansion velocities up to 100 km s^{-1} for a period of 10^4 y were estimated in a model involving the coupling between the rapid rotational motion of a protostellar envelope with a strong, circumstellar magnetic field (38).

5. Anisotropy

A growing number of observations indicate that the spatial distribution of outstreaming and/or swept-up, high velocity gas deviates from spherical symmetry. Fig. 6 shows the distribution of $J=1 \rightarrow 0$ CO emission in the dark cloud L1551 (39). The (R, v) -diagram on the left side clearly shows that the emission in the blueshifted and redshifted wings of the line are displaced from each other, while CO emission near line center (the "quiescent" gas) is present everywhere in the cloud. The "high" velocity CO gas appears to expand in two opposite lobes at a velocity of about 15 km s^{-1} (schematically shown on the right side). At the center of the CO cloud, a compact infrared source (IRS5) of low luminosity has been detected ($L \sim 30 L_{\odot}$) (40). Also present in the SW (the blueshifted) lobe are two Herbig-Haro objects, whose proper motions indicate that they expand away from IRS5 at $\sim 150 \text{ km s}^{-1}$ (41). Hence, Herbig-Haro objects, similar to H_2O masers, appear to be decelerating or accelerating cloudlets in the outflow, while the CO plateau comes from swept-up gas at the interface between flow and surrounding cloud.

"Bipolar" or at least anisotropic outflow appears to be typical also for other sources where sufficient spatial resolution is available. The proper motions of the Herbig-Haro objects 1 and 2, for example, suggest an outflow at 200 to 400 km s^{-1} in opposite directions away from a buried T-Tau star (42). A VLBI map of the most spectacular H_2O maser source in the Galaxy, W49, shows a clear separation between blue-shifted and redshifted high velocity maser features (43). In other maser sources, there is often a strong imbalance between the numbers or intensities of blue- and redshifted high velocity features in the H_2O spectra themselves (44-47). Finally, a large percentage of CO plateau sources discovered in recent surveys show a spatial offset between the centroids of blue- and redshifted emission (48-50).

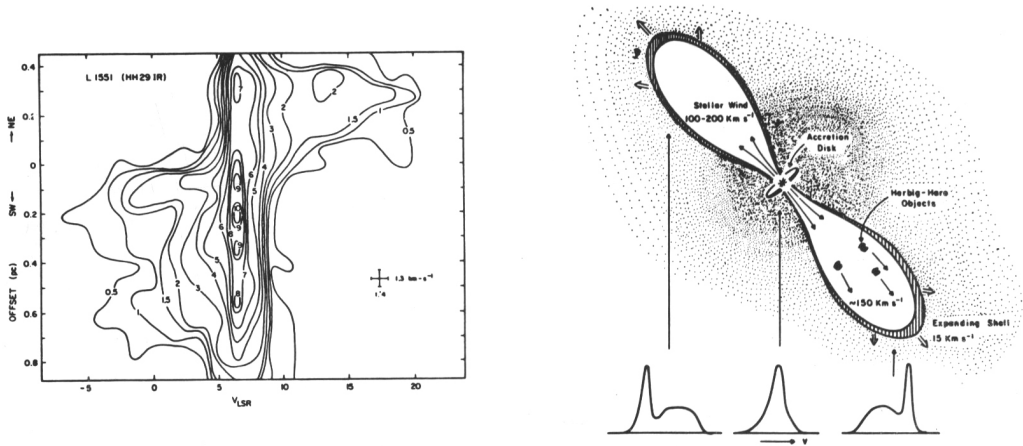


Fig. 6: The CO lobes in L1551 (39). Left: Velocity distribution of the $J=1-0$ line emission along the major axis of the cloud indicating that the emission in the blue- and redshifted CO wings is separated by about 1 pc. Right: Schematic diagram of the bipolar outflow and the Herbig-Haro objects expanding from the infrared source IRS5 (40, 41).

6. Later Stages

Mass outflow has also been found in young stars which are surrounded by compact, ionized regions. The widths of Brackett recombination lines at 2 and 4 μm toward several bright infrared sources indicate gas motions up to 100 km s^{-1} , suggestive of ionized winds from the stellar surfaces (52, 53). The emission measure of the high velocity gas toward the BN object in Orion, for example, together with the size of its radio HII region ($\sim 5 \times 10^{14} \text{ cm}$) (54), may indicate a mass loss rate of $\leq 10^{-6} M_{\odot} \text{ y}^{-1}$ (34). Note that this current mass loss rate is at least three orders of magnitude too small to make a significant contribution to the outflowing gas at the center of Orion-KL. The presence and scale sizes of the ionized regions, together with their luminosities and infrared appearances, suggest that "BN type" objects are young hot stars with a substantial ionizing luminosity, and which are still embedded in a dense envelopes at radii $\geq 10^{15} \text{ cm}$ from the stars.

III. Characteristics of an outflow region: Orion-IRc2

Because of its proximity and high luminosity, Orion-KL has become the "standard laboratory" for the investigation of the outflow phenomenon. Spectroscopic results from many lines between 1 μm and 10 cm wavelength, and investigations at arcsec resolution with large infrared telescopes as well as radio interferometers give a detailed picture of the outflow zone over three orders of magnitude in radius (10^{14} to 10^{17} cm). In the following, the results are summarized, and shown schematically in Fig. 7 in form of three "sketches", in order of increasing radius from the central stars

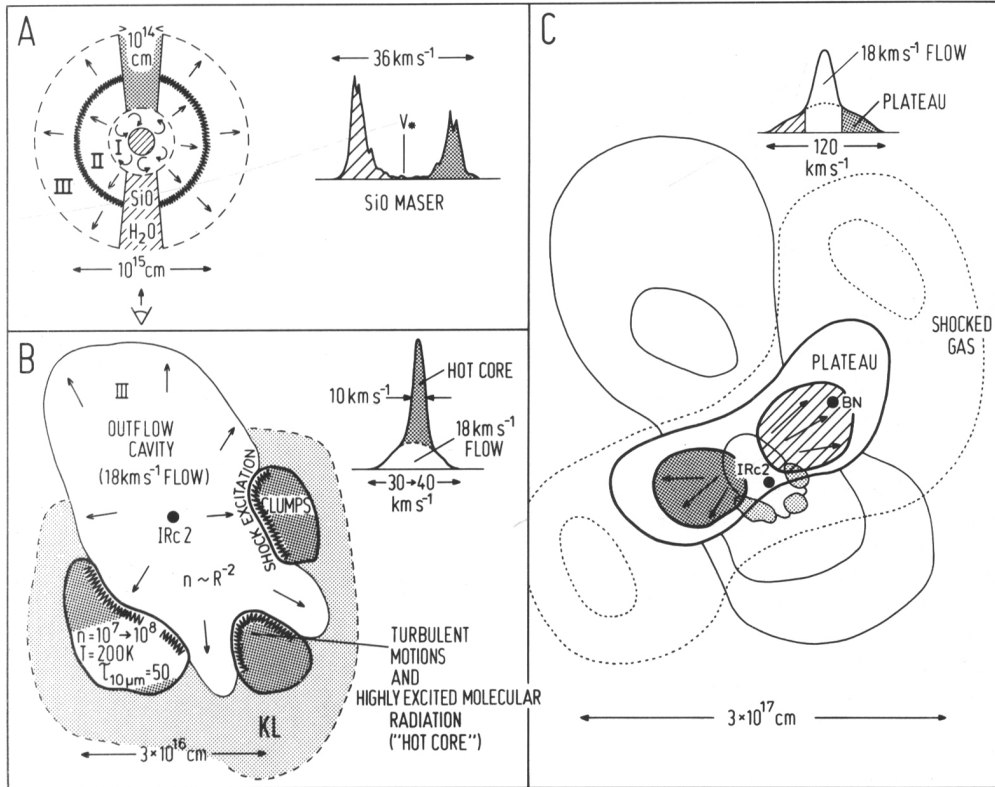


Fig. 7: Schematic diagram of the outflow zone around Orion-IRc2 (see text for references). Top left: The inner outflow region around IRc2. Region I ($< 10^{14}$ cm) may be a dust-free zone with mainly turbulent motions. SiO and H₂O maser radiation (see profile) comes from regions II and III. The double-peaked profile suggests that the outflow is at almost constant velocity ($12 \leq v \leq 18 \text{ km s}^{-1}$, the "18 km s⁻¹ flow") at $R > a$ few 10^{14} cm. The emission in the blueshifted (shaded) and redshifted (stippled) peaks probably comes from the front and back sides of the expanding envelopes, along the line of sight to the star. Bottom left: The outflow cavity and the interaction of the "18 km s⁻¹" flow with the surrounding cloud. The free flow extends out to about 3×10^{16} cm. Observations of highly excited molecular lines indicate the presence of knots of dense and warm gas (densely stippled), embedded in the KL nebula (light stipples). The flow may be stopped at the interface to these knots, creating turbulent gas which is observed as a "hot core" component in molecular line emission. Right: The high velocity zone. Outside of the "18 km s⁻¹ flow" cavity and the "hot core" region (schematically shown at the center), one finds high velocity gas with a velocity dispersion $> 100 \text{ km s}^{-1}$ (plateau, see profile at top). The heavy contours show that the high velocity flow is centered within a few arcsec of IRc2, but that blueshifted (shaded) and redshifted (stippled) wings are displaced from each other in NW-E direction. The dotted contours give the distribution of hot molecular hydrogen (shocked gas), and thin solid contours the contours of the quiescent molecular gas.

1) $R \leq 10^{14}$ to 10^{15} cm (Regions I and II, Fig. 7A)

Maser emission from vibrationally excited states of SiO comes from a region of a few 10^{14} cm in diameter, identical in position with the compact infrared source IRC2 to within $\pm 0.4''$ (33, 55, 56). The spectrum shown schematically in Fig. 7A, is double-peaked, with a separation of ~ 24 km s $^{-1}$ between the most intense features, and a total velocity range of 35 ± 3 km s $^{-1}$. Such a profile can be best explained by radiative transport of the maser radiation in an expanding (or contracting) envelope with small radial velocity gradients. In this case, the most favorable amplification paths come from the front and back sides of the envelope, along the line of sight to the star. The SiO data then suggest that there is an outflow at a low expansion velocity ($v_{\text{ex}} \sim 18$ km s $^{-1}$, the "18 km s $^{-1}$ " flow) which is fully developed and at almost constant velocity at $R > \text{a few } 10^{14}$ cm from IRC2 region II. A theoretical model of the SiO maser (57) requires that hydrogen densities in this zone are 10^{10} to 10^{11} cm $^{-3}$, and gas temperatures are about 1500 K. In this model, the radius of dust condensation ($\sim 10^{14}$ cm) is identical with the inner boundary of the maser zone. Inside of this radius (Region I), the motions may be chaotic (turbulent). Radiation pressure on dust then converts the turbulent motions into expansion between Regions I and II. Since the infrared opacities of dust are high in Region II, gas temperatures must be higher than dust temperatures in order not to thermalize the molecular levels and quench the maser action. A possible source of the high gas temperatures may be the dissipation of the turbulent motions.

2) $R = 10^{15}$ to 3×10^{16} cm (Region III, Fig. 1A, B)

In this region (the "outflow cavity"), the outflow velocity remains about constant ($12 \leq V \leq 18$ km s $^{-1}$), and the density may decrease according to R^{-2} . With increasing radius, molecular radiation is observed in order of decreasing excitation levels: H $_2$ O masers at $\sim 10^{15}$ cm, OH masers at $\geq 10^{16}$ cm, non-maser SiO emission out to a few 10^{16} cm (58-61). The inner boundary of this zone is coincident with the infrared photosphere, where the dust opacity becomes about unity between 2 and 10 μm ($T_{\text{d}} \sim 400$ K, 33). Out to the outer radius of the outflow cavity (3 to 5×10^{16} cm), the characteristics of the expanding envelope of IRC2 are very similar to those of late-type, evolved giants and supergiants (c.f. 62, 63).

3) $R = 3 \times 10^{16}$ to 3×10^{17} cm (Region IV, Fig. 7B, C)

In contrast to the envelopes of late-type stars, however, at $R = 3$ to 5×10^{16} cm the flow in Orion-KL encounters the surrounding molecular cloud with embedded, dense clumps. Observations of highly excited NH $_3$, HC $_3$ N, CH $_3$ CN and CH $_3$ OH lines indicate the presence of turbulent knots (diameter $\sim 10^{16}$ cm) of very dense ($n_{\text{H}_2} \geq 10^7$ cm $^{-3}$) and warm gas ($T \sim 200$ K, the "hot core", 64-71). A probable explanation is that the "18 km s $^{-1}$ " outflow is stopped there and that turbulent gas is excited by shock waves set up at the interface between flowing and stationary material. Hydrogen column densities through these knots are in excess of 10^{24} cm $^{-2}$, making the knots highly optically thick even at 10 to 30 μm

($\tau_{10\mu\text{m}} \geq 10$, $A_V \geq 300$, 66). The abundance of NH_3 molecules in the "hot core" region is much higher than in cool interstellar clouds, consistent with current models of shock chemistry (66, 67).

Fig. 7C schematically gives the distribution of the gas at $R > 3 \times 10^{16}$ cm. On this spatial scale, there is also gas with velocities $> 20 \text{ km s}^{-1}$ (the high velocity flow in addition to the " 18 km s^{-1} " flow discussed so far. The centroid of the $v=0$, $J=2 \rightarrow 1$ SiO "plateau" emission (72; see the schematic profile in Fig. 7C) is within a few arcsec of IRC2 (61, 72-73). However, the emission in the blueshifted wing is mainly to the NW, and the emission in the redshifted wing is to the E of IRC2 (heavy contours). The CO "plateau" emission has the same "bipolar" structure, but is of larger spatial extent ($\sim 30'' = 2 \times 10^{17}$ cm) and its centroid appears to be $5''$ to $10''$ north of IRC2 (74-76). Finally, the lobes from hot molecular hydrogen (dashed) also are to the NW and E of the center of the infrared cluster (14). All these observations suggest that the high velocity flow may also originate close to IRC2, but then preferentially streams NW and E, roughly perpendicular to the main ridge of the dense, quiescent molecular cloud (indicated by thin contours, from 77). The low velocity H_2O masers in the " 18 km s^{-1} " flow, on the other hand, appear to expand preferentially along the ridge (Fig. 5).

The high velocity outflow may be a second, independent flow and come from a source close to, but not coincident with IRC2. However, an alternative scenario is that there is originally only one — the " 18 km s^{-1} " — outflow from IRC2. This flow has cleared a cavity of radius 3 to 5×10^{16} cm around the central star. Further out, it is decelerated or even stopped ("hot core") along the dense ridge of the Orion molecular cloud. Perpendicular to the ridge, density gradients may be very steep ($n \sim R^{-\alpha}$, with $\alpha > 2$), and the flow may accelerate again, similar to the situation in a Laval nozzle, and then be observed as a second, high velocity flow (77, 177). This scenario may be supported by recent theoretical calculations (78-79), and by the fact that the momenta contained in the two flows are comparable (73). A strong influence of the surrounding molecular cloud on the shape and kinematics of the outflowing gas has also been suggested to account for the characteristics of the outflowing gas in Cep A (80).

There is currently no observational support for yet a third possibility: that the initial flow is at high velocities, but is then slowed down in the molecular cloud to velocities $\leq 20 \text{ km s}^{-1}$. As mentioned above, the " 18 km s^{-1} " flow can be traced to the inner envelope of IRC2, and there is no evidence for higher velocity material on a spatial scale $< 10^{16}$ cm.

4) Evolutionary state of IRC2

Recent measurements of the near infrared polarization have strongly supported the suggestion (33), that IRC2 is the dominant heating source in the infrared cluster, with an intrinsic luminosity close to $10^5 L_\odot$, the total far-infrared luminosity of the Orion-KL region (83). Its

relative weakness on the near-infrared maps is most likely caused by extinction by dust in one of the "hot core" clumps. Because of the large foreground obscuration, little is known about conditions close to the stellar surface and hence, about the evolutionary state of the star. As mentioned above, the surface temperature must be in excess of a few thousand degrees, to account for the SiO masers. The current data do not rule out the possibility that IRC2 is an evolved, post-main sequence supergiant (84). Nevertheless, indirect arguments favor the idea that IRC2 is a young hot star on its way to the main sequence (33): IRC2 is located at the center of a dense molecular cloud and is close to the BN object which is almost certainly a young B star. There is no evidence for an extended HII region, and the mass loss rate of IRC2 appears to be higher than is typical for supergiants of comparable luminosity. Finally, there are mass-loss objects similar to IRC2 in many regions of star formation, over a wide range in luminosity.

IV STATISTICAL RESULTS

Detailed observations of a growing number of sources suggest that H₂O masers and Herbig-Haro objects, non-Gaussian wings in molecular and atomic lines, and emission from highly excited gas, are all probably independent manifestations of activity caused by mass outflows at the centers of dense, interstellar clouds. From the data in about 20 "plateau" sources (e.g. 48-51, 80-83), 200 maser sources (e.g. 45-47, 85-88), and from surveys for H₂-quadrupole and Brackett recombination lines (e.g. 36,53, 89-91), the following statistical conclusions can be drawn.

- 1) "Activity" can be found in almost all regions of recent star formation, covering a range of five orders of magnitude in luminosity. In many cases, the outflow appears to come from a T-Tau star, a compact infrared continuum source or an ultra-compact H II region embedded in a molecular cloud. Violent mass loss at velocities between 10 and 300 km s⁻¹ seems to be common in all newly-formed stars more massive than a few M_⊙. The expanding flows are associated with an early stage of stellar evolution, before the young stars have reached the main sequence, or have had time to develop substantial H II regions.
- 2) The outflow zones have diameters between 0.01 and a few pc, and dynamical time scales are $\leq 10^4$ yr. From the counts of H₂O masers and a statistical comparison of their occurrence with the galactic star formation rate, or the lifetimes of compact H II regions, the duration of the H₂O maser phase has been estimated to be between 10⁴ and 10⁵ y (85, 92).

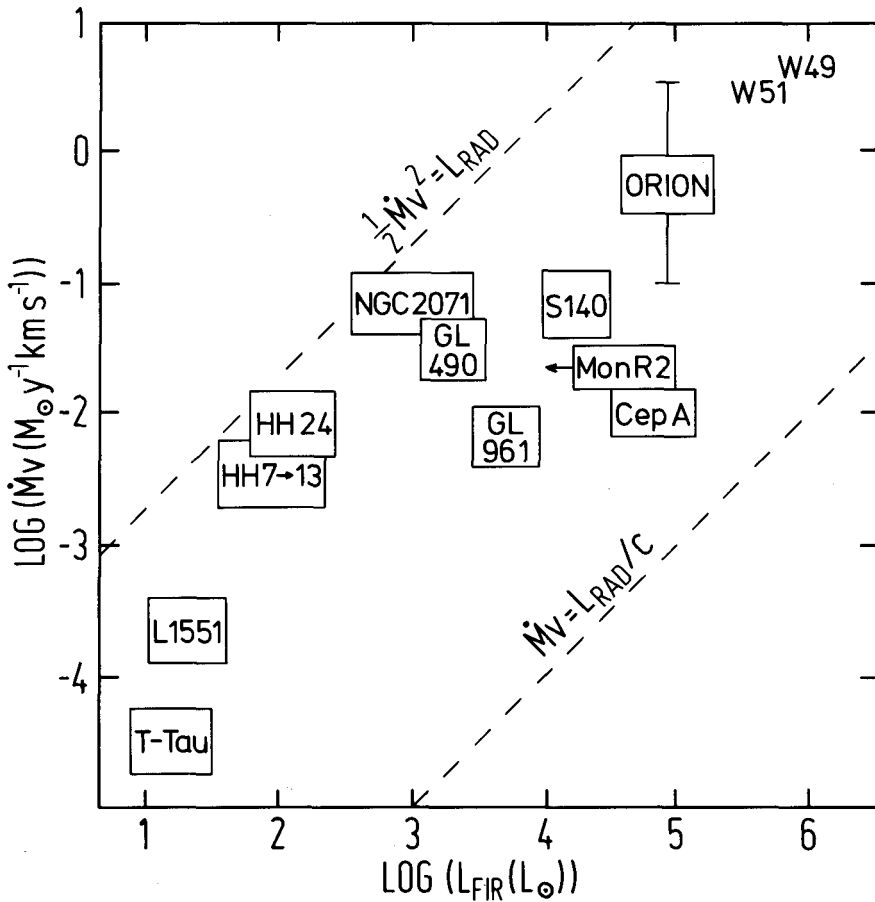


Fig. 8: Momentum in the outflowing/swept-up gas vs. total infrared luminosity (from 48, 49 and 73), for 13 outflow sources. A typical error bar is shown, for Orion. The dashed lines indicate (i) momentum of the flow equal to that of the radiation field ($\dot{M}v = L_{RAD}/c$), and (ii) mechanical energy equal to radiated luminosity ($\frac{1}{2}\dot{M}v^2 = L_{RAD}$).

3) Fig. 8 is a plot of momentum in the flows vs. total infrared luminosity of the regions (from CO data in (48, 49), with addition of W 49 and W 51, where SiO plateau emission has been detected (73)). Despite the uncertainties, the data suggest an increase of flow momentum with total IR luminosity. The momentum in the flows is generally >ten times larger than can be driven by radiation pressure,

with single scattering. However, the data in Fig. 8 do not yet prove a physical correlation between mass loss and luminosity, for two reasons: (i) The luminosity of the outflow source in each region may be only a small fraction of the total (cluster) luminosity. (ii) Objects toward the upper right of the diagram are also more distant, and the observed high velocity wings are often only a few times the noise limit. Hence, the apparent good correlation may be severely influenced by detectability, combined with a Malmquist bias.

- 4) The flowing and /or swept-up, high velocity gas appears to be distributed anisotropically over size scales of 10^{16} to 10^{18} cm. It is currently not clear whether the flows are always collimated into two narrow, opposite lobes (jets), as suggested by the observations in L1551 and HH 1/2, or whether the general pattern is more irregular, such as a channeling of an intrinsically isotropic flow by more or less random gradients and density inhomogeneities in the surrounding cloud. A collimated outflow very close to the central star probably requires an anisotropic mass loss mechanism (see 38), or the presence of a thick circumstellar disk.

V IMPACT ON SURROUNDING MOLECULAR CLOUDS

1) Core of Orion-KL

The total mass in the central 1' to 2' of the Orion-KL region is $\sim 200 M_{\odot}$. If the molecular linewidths of $\sim 3 \text{ km s}^{-1}$ are caused by small-scale "turbulence" in the quiescent gas, the total energy in these turbulent motions is about 10^{46} erg. This is comparable with the total gravitational energy, but is about an order of magnitude larger than the thermal energy in the core of the molecular cloud. Since the mechanical energy in the outflow is about 5×10^{47} erg, the mass motions from the center of the IR cluster could easily account for the observed "turbulent" broadening of molecular lines, from the "quiescent" gas, and support this gas against gravitational collapse (c.f. 1, 31, 48).

2) Galactic Scale

Apart from the possible bias in the available observations, the data shown in Fig. 8 suggest that the mechanical power in the high velocity flows (L_{HVF}) is a substantial fraction of the total luminosity (L_{tot}) of the central stars (a fit to the data gives $L_{\text{HVF}} \sim 2 \times 10^{-2} L_{\text{tot}}$, ref. 48). The total mechanical energy delivered per mass interval of newly formed stars per sec, integrated over the duration of the mass loss phase (t_{HVF}) is then (48):

$$\Lambda_{\text{HVF}}(M) = L_{\text{HVF}}(M) t_{\text{HVF}}(M) \rho(M) \quad (\text{erg s}^{-1}),$$

where $\rho(M)$ is the number of stars formed in the Galaxy per sec in the mass interval $(M, M+dM)$. If $\rho(M) \sim M^{-2.5}$ (48), and $L_{\text{HVF}} \sim L \sim M^{3.3}$ (appropriate for main sequence stars), then O and B-type stars make the major contribution, provided t_{HVF} does not decrease faster than about M^{-1} .

If one assumes, for example, a mass-independent time scale ($t_{\text{HVF}} = 10^4$ to 10^5 yr), the total energy input of all stars can be integrated, with a suitable form of ρ (ref 93) to yield (48):

$$\int_{\text{a few } M_{\odot}}^{\infty} \Lambda_{\text{HVF}}(M) dM \sim 10^{38} \text{ to } 10^{39} \text{ erg s}^{-1}$$

A value of the same magnitude may be obtained if one assumes instead that all stars lose a certain percentage (10 to 50 %) of their initial mass by the outflow processes (1, see also 98). In this case, the least massive stars (T-Tau etc) contribute most because of their larger numbers.

On a galactic scale, this energy input is much smaller than that estimated from supernova explosions and winds of main-sequence OB stars (~ 2 to 7×10^{41} erg s^{-1} , 94). On smaller scales, however, the outflows from young stars may nevertheless be important for the support of molecular clouds. For a total mass in molecular gas of $2 \times 10^9 M_{\odot}$ and a typical "turbulent" velocity of 1 km s^{-1} , the total mechanical energy in dense interstellar clouds is $\sim 3 \times 10^{52}$ erg. This energy can be provided by the outflows over a time scale of 10^6 to 10^7 yr, comparable with the free-fall time scale of the clouds (48).

Acknowledgements Most of this review was written while R.G. was visiting the Max-Planck-Institut für Radioastronomie, Bonn. R.G. is grateful to P.G. Mezger and the institute staff for help and hospitality.

REFERENCES

1. Genzel, R. and Downes, D. 1982, in "Regions of Recent Star Formation", eds. R.S. Roger and P.E. Dewdney, Reidel, pp 251.
2. Bally, J. and Lada, C. 1982, preprint.
3. Lada, C. 1982, Bull. AAS 14, 641.
4. Sullivan, W.T. 1973, Ap. J. Suppl. 25, 393.
5. Strel'nitskii, V. and Syunyaev, R. 1972, Astron. Zh. 49, 704; Sov. Astron. 16, 579 (1973).
6. Kwan, J. and Scoville, N. 1976, Ap. J. 210, L39.
7. Zuckerman, B., Kuiper, T. and Rodriguez-Kuiper, E. 1976, Ap. J. 209, L137.
8. Wilson, R.W., Jefferts, K.B. and Penzias, A.A. 1970, Ap. J. 161, L43.
9. Thaddeus, P., Kutner, M., Penzias, A., Wilson, R. and Jefferts, K. 1972, Ap. J. 176, L73.
10. Dickinson, D. 1972, Ap. J. 175, L43.
11. Herbig, G.H. 1951, Ap. J. 113, 697.
12. Haro, G. 1952, Ap. J. 115, 572.
13. Gautier, T., Fink, U., Treffers, R. and Larson, H. 1976, Ap. J. 207, L129.

14. Beckwith, S., Persson, E., Neugebauer, G. and Becklin, E. 1978, Ap. J. 223, 464.
15. Simon, M., Righini-Cohen, G., Joyce, R. and Simon, T. 1979, Ap. J. 230, L175.
16. Beck, S., Lacy, J., and Geballe, T. 1979, Ap. J. 234, L213.
17. Knacke, R. and Young, E. 1981, Ap. J. 249, L65.
18. Scoville, N. Kleinmann, S., Hall, D. and Ridgway, S. 1981, Ap. J. 253, 136.
19. Beckwith, S., Evans, N., Gatley, I., Gull, G. and Russell, R. 1982, in press.
20. Davis, D.S., Larson, H.P. and Smith, H.A. 1982, Ap. J. 259, 166.
21. Nadeau, D., Geballe, T. and Neugebauer 1982, Ap. J. 253, 154.
22. Watson, D., Storey, J., Townes, C., Haller, E., and Hansen, W. 1980, Ap. J. 239, L129.
23. Storey, J., Watson, D., Townes, C., Haller, E. and Hansen, W. 1981, Ap. J. 247, 136.
24. Watson, D. 1982, Ph. D. Thesis, University of California, Berkeley.
25. Kwan, J. 1977, Ap. J. 216, 713.
26. London, R., McCray, R., and Chu, S.I. 1977, Ap. J. 217, 442.
27. Draine, B. 1980, 241, 1021.
28. Chernoff, D.F., Hollenbach, D.J. and McKee, C.F. 1982, Ap. J. 259, L97.
29. Draine, B. and Roberge, W. 1982, Ap. J. 259, L91.
30. Knapp, G., Phillips, T., Huggins, P. and Redman, R. 1981, Ap. J. 250, 175.
31. Solomon, P., Huguenin, G. and Scoville, N. 1981, Ap. J. 245, L19.
32. Genzel, R., Reid, M., Moran, J. and Downes, D. 1981, Ap. J. 244, 884.
33. Downes, D., Genzel, R., Becklin, E. and Wynn-Williams, C.G. 1981, Ap. J. 244, 869.
34. Zuckerman, B. in IAU Symp. No. 96, Infrared Astronomy, eds. C. Wynn-Williams and D. Cruikshank, Reidel, p.275.
35. Scoville, N. *ibid*, p.187.
36. Beckwith, S. *ibid*, p.167.
37. Phillips, J. and Beckman, J. 1980, MNRAS 193, 245.
38. Hartmann, L. and McGregor, K. 1982, Ap. J. 259, 180.
39. Snell, R., Loren, R. and Plambeck, R. 1980, Ap. J. 239, L17.
40. Beichman, C. and Harris, S. 1981, Ap. J. 245, 589.
41. Cudworth, K. and Herbig, G. 1979, A.J. 84, 548.
42. Herbig, G. and Jones, B. 1981, A.J. 86, 1232.
43. Walker, R.C., Matsakis, D. and Garcia-Barreto, J. 1982, Ap. J. 255, 128.
44. Heckman, T. and Sullivan, W. 1976, Ap. Lett. 17, L105.
45. Morris, M. 1976, Ap. J. 210, 100.
46. Genzel, R. and Downes, D. 1977, Astr. Ap. Suppl. 30, 145.
47. Goss, W.M., Knowles, S., Balister, M., Batchelor, R. and Wellington, K. 1976, MNRAS 174, 541.
48. Bally, J. and Lada, C. 1982, preprint.
49. Rodriguez, L., Carral, P., Ho, P., and Moran, J. 1982, Ap. J. 260, 635.
50. Snell, R. and Edwards, S. 1982, in press.

51. Blitz, L. and Thaddeus, P. 1980, *Ap. J.* 241, 676.
52. Hall, D., Kleinmann, S., Ridgway, S. and Gillett, F. 1978, *Ap. J.* 223, L47.
53. Simon, M. et al. 1982, preprint.
54. Moran, J.M., Garay, G., Reid, M., Genzel, R. and Ho, P. 1982, in *Proc. of the Symposium on Orion Nebula to Honor H. Draper*, eds. A. Glassgold and P. Huggins, New York Academy of Sciences.
55. Genzel, R., Moran, J., Lane, A., Predmore, C., Ho, P., Hansen, S. and Reid, M. 1979, *Ap. J.* 231, L73.
56. Wright, M. and Plambeck, R., in prep.
57. Elitzur, M. 1982; *Ap. J.* in press.
58. Hansen, S. 1980, Ph.D. Thesis, Univ. of Mass.
59. Hansen, S. and Johnston, K. 1980, *Bull. AAS* 12, 824.
60. Genzel, R., Downes, D., Schwartz, P., Spencer, J., Pankonin, V. and Baars, J. 1980, *Ap. J.* 239, 519.
61. Plambeck, R., priv. comm.
62. Snyder, L. 1980, in *IAU Symp. 87, Interstellar Molecules*, ed. B. Andrew, Reidel.
63. Reid, M. and Moran, J. 1981, *Ann. Rev. Astr. Ap.* 19, 231.
64. Wilson, T., Downes, D. and Bieging, J. 1979, *Astr. Ap.* 71, 275.
65. Morris, M., Palmer, P. and Zuckerman, B. 1980, *Ap. J.* 237, 1.
66. Genzel, R., Downes, D., Ho, P. and Bieging, J. 1982, *Ap. J.* 259, L103.
67. Bieging, J., Martin, R., Pauls, T. and Wilson, T. 1982, in prep.
68. Clark, F., Brown, R., Godfrey, P., Storey, J., and Johnson, R. 1976, *Ap. J.* 210, L139.
69. Loren, R., Erickson, N., Snell, R., Mundy, L. and Davis, J. 1981, *Ap. J.* 244, L107.
70. Goldsmith, P., Snell, R., Deguchi, S., Krotkov, R. and Linke, R. 1982, *Ap. J.* 260, 147.
71. Hollis, J. M., Lovas, F.J., Suenram, R.D., Jewell, P.R., Snyder, L.E. 1982, *Ap. J.*, in press.
72. Olofsson, H., Hjalmarsen, A. and Rydbeck, O. 1981, *Astr. Ap.* 100, L30.
73. Downes, D., Genzel, R., Hjalmarsen, A., Nyman, L.A. and Rönnäng, B. 1982, *Ap. J.* 252, L29.
74. Erickson, N., Goldsmith, P., Ulich, B., Lada, C., Berson, R., Snell, R. and Huguenin, C. 1982, *Bull. AAS* 14, 627.
75. Phillips, J.P., White, G. and Watt, G. 1982, *MNRAS* 199, 1033.
76. Olofsson, H., Ellender, J., Hjalmarsen, A. and Rydbeck, G., preprint.
77. Plambeck, R., Wright, M., Welch, W., Bieging, J., Baud, B., Ho, P. and Vogel, S. 1982, *Ap. J.* 259, 617.
78. König, A. preprint.
79. Canto, J. 1980, *Astr. Ap.* 86, 327.
80. Ho, P., Moran, J. and Rodriguez, L. 1982, *Ap. J.* in press.
81. Lada, C., and Harvey, P. 1981, *Ap. J.* 245, 58.
82. Barrett, J. and Solomon, P. 1982, in prep.
83. Werner, M., Dinerstein, H. and Capps, R. 1982, *Ap. J.* Submitted.
84. Snyder, L. and Buhl, D. 1974, *Ap. J.* 189, L31.
85. Genzel, R. and Downes, D. 1979, *Astr. Ap.* 72, 234.

86. Goss, W.M., Haynes, R., Knowles, S., Batchelor, R. and Wellington, K. 1977, *MNRAS*, 180, 51p.
87. Rodriguez, L., Moran, J., Ho, P. and Gottlieb, E. 1980, *Ap. J.* 235, 845.
88. Batchelor, R., Caswell, J., Goss, W.M., Haynes, R., Knowles, S., and Wellington, K. 1980, *Austr. J. Phys.*, 33, 139.
89. Fisher, J., Righini-Cohen, G., Simon, M., Joyce, R. and Simon, T. 1980, *Ap. J.* 240, L95.
90. Thompson, R. 1982, *Ap. J.* 257, 171.
91. Bally, J. and Lane, A. 1982, *Ap. J.* in press.
92. Jaffe, D., Güsten, R. and Downes, D. 1981, *Ap. J.* 250, 621.
93. Miller, G. and Scalo, J. 1979, *Ap. J. Suppl.* 41, 513.
94. Spitzer, L. 1978, "Physical Processes in the Interstellar Medium", Wiley.
95. Goldsmith, P., Erickson, N., Fetterman, H., Clifton, B., Peck, B., Tannenwald, P., Koepf, G., Buhl, D. and McAvoy, N. 1981, *Ap. J.* 243, L79.
96. van Vliet, A., de Graauw, Th., Lee, T., Lidholm, S. and v. d. Stadt, H. 1981, *Astr. Ap.* 101, L1.
97. Stacey, G., Kurtz, N.T., Smyers, S., Harwit, M., Russell, R. and Melnich, G. 1982, *Ap. J.* 257, L37.
98. Norman, C. and Silk, J. 1979, *Ap. J.* 228, 197.